The effect of the cyclin-dependent kinase inhibitor flavopiridol on anaplastic large cell lymphoma cells and relationship with NPM-ALK kinase expression and activity

Paolo Bonvini, Elisa Zorzi, Lara Mussolin, Giovanni Monaco, Martina Pigazzi, Giuseppe Basso, and Angelo Rosolen

Clinica di Oncoematologia Pediatrica, Azienda Ospedaliera-Università di Padova, Italy

ABSTRACT

Background

The loss of cell cycle regulation due to abnormal function of cyclin-dependent kinases (cdk) occurs in tumors and leads to genetic instability of chemotherapy-resistant cells. In this study, we investigated the effect of the cdk inhibitor flavopiridol in anaplastic large cell lymphomas, in which unrestrained proliferation depends on NPM-ALK tyrosine kinase activity.

Design and Methods

Effects of flavopiridol were examined in ALK-positive and -negative anaplastic large cell lymphoma cells by means of immunoblotting and immunofluorescence analyses to assess cdk expression and activity, quantitative real time reverse transcriptase polymerase chain reaction to measure drug-induced changes in transcription, and FACS analyses to monitor changes in proliferation and survival.

Results

Treatment with flavopiridol resulted in growth inhibition of anaplastic large cell lymphoma cells, along with accumulation of subG$_1$ cells and disappearance of S phase without cell cycle arrest. Consistent with flavopiridol activity, phosphorylation at cdk2, cdk4, cdk9 sites on RB and RNA polymerase II was inhibited. This correlated with induction of cell death through rapid mitochondrial damage, inhibition of DNA synthesis, and down-regulation of anti-apoptotic proteins and transcripts. Notably, flavopiridol was less active in ALK-positive cells, as apoptosis was observed at higher concentrations and later time points, and resistance to treatment was observed in cells maintaining NPM-ALK signaling. NPM-ALK inhibition affected proliferation but not survival of anaplastic large cell lymphoma cells, whereas it resulted in a dramatic increase in apoptosis when combined with flavopiridol.

Conclusions

This work provides the first demonstration that targeting cdk is effective against anaplastic large cell lymphoma cells, and proves the critical role of NPM-ALK in the regulation of responsiveness of tumor cells with cdk dysregulation.

Key words: anaplastic large cell lymphoma, NPM-ALK, cell cycle.

Citation: Bonvini P, Zorzi E, Mussolin L, Monaco G, Pigazzi M, Basso G, and Rosolen A. The effect of the cyclin-dependent kinase inhibitor flavopiridol on anaplastic large cell lymphoma cells and relationship with NPM-ALK kinase expression and activity. Haematologica 2009;94:944-955. doi:10.3324/haematol.2008.004861

Funding: this research was funded by Fondazione Città della Speranza and by MIUR (Ministero Istruzione Università e Ricerca).

Acknowledgments: the authors would like to thank S. Disarò and Dr. C. Frasson (Dept. of Pediatrics, University of Padova, Italy) for the flow cytometry analysis; and Dr. Leonard M. Neckers (Urologic Oncology Branch, NCI, Bethesda, MD, USA) for critical review of the manuscript.

Manuscript received on December 19, 2008. Revised version arrived on February 12, 2009. Manuscript accepted on March 2, 2009.

Correspondence:
Paolo Bonvini, Ph.D., Clinica di Oncoematologia Pediatrica, Azienda Ospedaliera-Università di Padova, via Giustiniani 3, 35128 Padova, Italy.
E-mail: paolo.bonvini@unipd.it

The online version of this article contains a supplementary appendix.

Introduction

Cyclin-dependent kinases (cdk) are a family of serine/threonine kinases that, in complex with cyclins, regulate cell cycle progression. Unlike cyclins, which fluctuate to ensure proper timing of complex formation, cdk remain stable during the cell cycle but their activation is transient due to rapid downregulation of cyclins or changes in their phosphorylation state.[1] Four of the cdk so far identified are active during the cell cycle (cdk1, cdk2, cdk4 and cdk6), one acts as an activating kinase for the others (cdk7), and three are involved in transcriptional regulation (cdk7, cdk8 and cdk9). In association with cyclins D, E and A, cdk4/6 and cdk2 govern G_1- and S-phase progression respectively, through sequential phosphorylation of retinoblastoma tumor suppressor protein (RB) and E2F1 transcription factor,[2] whereas the cyclin B1-cdk1 complex promotes G_2-phase traversal and exit from mitosis.[3] In complex with cyclins H and T, cdk7 and cdk9, instead, act as direct regulators of the transcriptional machinery, promoting initiation and elongation of nascent transcripts through phosphorylation of the RNA polymerase II enzyme.[4] Inhibition of cdk7/9 primarily affects general transcription and cell survival, whereas inhibition of cdk1, 2 and 4/6 accounts mostly for growth arrest or delay in phase progression.[5] Deregulated cdk activity is a hallmark of human cancer, and a variety of genetic and epigenetic events, such as overexpression of cyclins, diminished levels of cdk inhibitors or gain-of-function mutations in cdk, have been described to cause overactivity of these enzymes and provide a selective growth advantage in tumor cells.[6-8] This renders cdk suitable targets for anti-cancer therapy and has prompted great interest in the development of specific inhibitors.[9,10]

Flavopiridol is a semisynthetic ATP-competitive inhibitor of cdk,[11,12] capable of inducing either cell cycle arrest or apoptosis, through inhibition of cdk 1, 2 and 4/6, or cdk7 and 9, but without a direct effect on protein stability.[13,14] The primary response of tumor cells to flavopiridol is cytostatic growth arrest with delayed cytotoxicity, but cell cycle arrest and apoptosis may occur concomitantly, and cell death can be the preferential response. However, due to effects on multiple cellular targets and actions beyond cdk inhibition, flavopiridol has antitumor activity on a variety of cancer cells, but lacks an univocal mechanism of action that explains selective cell killing. Here, we studied the effect of flavopiridol and examined its potential mechanism of action on proliferation and survival of anaplastic large cell lymphomas (ALCL), a subset of T-cell lymphomas characterized by chromosomal translocations involving the *ALK* gene, which gives rise to the fusion oncoprotein NPM-ALK, characterized by constitutive active tyrosine kinase activity.[15,16] NPM-ALK signals through a multitude of downstream survival pathways (JAK/STAT, PI3K/AKT, RAS/ERK and JNK) and is responsible for the enhanced transcription and expression of several anti-apoptotic molecules, cell-cycle regulators, ribosomal proteins and transcription factors, as well as for the inactivation of their corresponding inhibitors (RB, $p21^{WAF}$, $p27^{Kip}$).[17] However, little is known about the effects of simultaneous interruption of survival signaling and cell cycle regulatory pathways on the behavior of ALCL cells, and cdk inhibitors have not been studied in ALCL nor have they been shown to modulate NPM-ALK signaling. We, therefore, studied the effects of flavopiridol on these aspects.

Design and Methods

Cell culture

Human ALK-positive ALCL cell lines Karpas299, SUDHL1, and ALK-negative FE-PD cells were maintained in RPMI 1640 medium containing 15% heat-inactivated fetal calf serum (FCS), 2 mmol/L glutamine, 100 U/mL penicillin, and 100 μg/mL streptomycin under standard tissue-culture conditions.

Reagents and antibodies

The cdk inhibitor flavopiridol (NSC 649890) was obtained from the Developmental Therapeutics Program (National Cancer Institute, NIH, Bethesda, MD, USA), dissolved in dimethylsulfoxide (DMSO) and stored at -80°C until use. WHI-154 was purchased from Calbiochem (Calbiochem, USA). Antibodies were purchased from Cell Signaling (PARP; E2F1; RB; cyclin B1; cdk2; cdk4: cdk7, cdk9; $STAT3^{Y705}$; Akt and Akt^{S472}; JNK and $JNK^{T183/Y185}$; ERK1/2 and $ERK1/2^{T202/Y204}$; p38α and $p38\alpha^{T180/Y182}$; NPM-ALK^{Y664}) (Cell Signaling Technology, Inc., USA); SIGMA (γ-tubulin; RB^{S780}; RB^{S612}; RB^{T821}) (SIGMA-Aldrich Co., USA); Calbiochem (cyclin E) (Oncogene Research Products, USA); Santa Cruz (Mcl-1; Bax [N20]; cytochrome-c [7H8.2C12]; cyclin D3; RNA Pol II; STAT3) (Santa Cruz Biotechnology, Inc., USA); BD Transduction laboratories ($p21^{WAF}$ and $p27^{KIP}$) (BD Biosciences Pharmingen, USA); Upstate (Bax [6A7]; Bak; cyclin A) (Upstate Biotechnology, NY, USA); Alexis (caspase-3) (Axxora Life Science, USA); Covance (RNA Pol II^{Ser2} [H5]) (Covance, CA, USA). Caspase inhibitor z-vad-fmk was purchased from Biomol (Biomol International LP, USA). PMSF was purchased from SIGMA (SIGMA-Aldrich Co., USA), whereas leupeptin and aprotinin protease inhibitors were obtained from CAPPEL (ICN Biomedicals Inc., USA). DAPI nucleic acid stain, fluorophore-conjugated goat anti-rabbit Alexa488 and goat anti-mouse Alexa546 antibodies were bought from Molecular Probes (Molecular Probes Inc., USA). Horseradish peroxidase-conjugated sheep anti-mouse and donkey anti-rabbit antibodies were purchased from GE Healthcare (GE Healthcare Bio-Sciences AB, Uppsala, Sweden), as were protein A-sepharose beads and protein G-sepharose Fast-Flow™ beads. The BCA protein assay was from PIERCE (Pierce Chemical Co., USA) while western blot chemiluminescence reagents were purchased from Chemicon (Chemicon International, Inc., USA). Nitrocellulose and PVDF membranes were from Schleicher & Schuell. All of the other chemicals used were purchased from SIGMA.

Cell viability assay

ALCL cell viability was assessed by MTT. Briefly, 0.1×10^6/mL cells were seeded in 96-well plates. The

cells were grown in the presence or absence of the drug at 37°C for up to 72 h and reduction of the MTT salt was measured every 24 h at 540 nM. MTT salt (3-(4,5-dimethylthiazol-2-yl)-2,5-diphenyltetrazolium bromide; SIGMA Co., USA) was added for 4 h. Values represent the mean (±SD) of triplicate cultures of three independent experiments. The median-effect dose (IC_{50}) was calculated using CalcuSyn software (Calcusyn, Biosoft, MO, USA) and applying Chou's median-effect equation.

Cell lysis, immunoblotting and immunoprecipitation

ALCL cells were treated with flavopiridol or left untreated as indicated. The cells were then washed twice in ice-cold 1x phosphate-buffered saline (PBS) and lysed by addition of TritonX-100 sample buffer (10 mM Tris-HCl [pH 7.5]; 130 mM NaCl; 1% TritonX-100; 5 mM EDTA; 1 mg/mL BSA; 20 mM sodium phosphate [pH 7.5]; 10 mM sodium pyrophosphate [pH 7.0]; 25 mM glycerophosphate; 1 mM sodium orthovanadate; 10 mM sodium molybdate; 1 mM PMSF; 20 μg/mL leupeptin; 20 μg/mL aprotinin). The lysates were clarified by high-speed centrifugation, and 30 μg of lysate were fractionated by sodium dodecylsulfate polyacrylamide gel electrophoresis (SDS-PAGE) and transferred to nitrocellulose. To assess processing and cleavage of caspase 3 flavopiridol-treated and untreated cells were lysed with 200 μL of urea-buffer [62.5 mM Tris-HCl, (pH 6.8); 6 M urea; 10% glycerol; 2% SDS; 5% β-mercaptoethanol]. Samples were prepared for western blotting as described above, and normalized for the expression of γ-tubulin. Proteins were visualized by chemiluminescence using a commercial kit (Chemicon). Immunoprecipitation was performed as described previously. Briefly, the cells were lysed as above, and 0.5 mg of protein lysates were precipitated, overnight at 4°C, with 1 μg specific primary antibodies. The immunocomplexes were adsorbed onto 30 μL protein G sepharose beads, incubated at 4°C for 120 min and then resuspended in sample buffer before fractionation by SDS gel electrophoresis. Western blotting was performed as above.

Assessment of apoptosis

After flavopiridol treatment and induction of apoptosis, 0.5×10^6 cells were harvested and washed with temperate PBS. The cells were resuspended in 1 mL of 1X annexin-binding buffer (10 mM HEPES, pH 7.4; 140 mM NaOH; 2.5 mM $CaCl_2$), stained with 5 μL annexin-V-fluorescein isothiocyanate (FITC) and 5 μl of 5 μg/mL propidium iodide (PI), and then incubated for 15 min at room temperature in the dark (Immunostep Research, Spain). The apoptotic cells were determined using a Beckam Coulter FC500 flow cytometer. Both early apoptotic (annexin-V-positive, PI-negative) and late (annexin-V-positive and PI-positive) apoptotic cells were included in cell death determinations.

BrdU analysis

Flavopiridol-treated and untreated cells (1×10^6) were pulse-labeled with 10 μM BrdU for 45 min before collection (FITC BrdU Flow Kit, BD Pharmingen). Briefly, after BrdU labeling the cells were washed in 1X DPBS, fixed in 4% paraformaldehyde and permeabilized with saponin detergent for 30 min on ice, according to the instructions provided with the kit. The cells were then treated with DNase for 1 h at 37°C, to expose incorporated BrdU, washed with 1X DPBS and stained with FITC-conjugated anti-BrdU antibody (1/50), for 20 min at room temperature. At the end, total DNA was stained with 7-amino-actinomycin D (7-AAD) fluorescent dye for 15 min at room temperature in the dark, and then, once resuspended in staining buffer, analyzed by two-color flow cytometry.

Real-time polymerase chain reaction

ALCL cells were untreated or treated with 200 nM flavopiridol for the indicated time periods. After treatment, the cells were lysed, and total RNA was isolated using Trizol (Invitrogen, Carlshad, CA, USA) following the manufacturer's instructions. Contaminating DNA was removed with a DNA-free™ Kit (AMBION Inc., USA) according to the manufacturer's instructions. One microgram of RNA was reverse transcribed using SuperScript II reverse transcriptase (Invitrogen) and random hexamers. The following primers and probe sequences were designed using Primer Express version 2.0 (Applied Biosystems) for TaqMan- based quantitative real-time polymerase chain reaction (RQ-PCR) experiments: human *Mcl-1*, forward 5'-TAAGGACAAAACGGGACTGG-3', reverse 5'-ACATTCCTGATGCCACCTTCTAG-3',Taqman probe 5'-FAM-CTGGGATGGGTTTGTGGAGTTCTTCCA-TAMRA-3'. The thermal cycler conditions were 2 min at 50°C for uracil N-glycosylase treatment and 10 min at 95°C for inactivation of uracil N-glycosylase and activation of AmpliTaq Gold Polymerase, followed by 50 cycles of 15 seconds at 95°C and 1 min at 60°C. All reactions were performed on the ABI Prism 7000 Sequence Detection System (Applied Biosystems, CA, USA). To compare RQ-PCR assays from different runs, the threshold was set at 0.1. To identify the most appropriate endogenous control gene for the quantification of Mcl-1 expression in ALCL cell lines, we conducted a preliminary expression analysis of 11 house-keeping genes in these cell lines, by RQ-PCR using 5' nuclease technology, and Human TaqMan® pre-developed assay reagent endogenous controls (ABI, Foster City, CA, USA). 18S was the best candidate control gene because its expression showed the lowest variability across the test samples. Each sample was tested in triplicate, and Mcl1 mRNA levels were normalized to that of 18s rRNA.

Subcellular fractionation

Lysates were obtained by resuspending ALCL cells in digitonin-lysis buffer [250 mM sucrose; 20 mM Hepes, (pH 7.4); 5 mM $MgCl_2$; 10 mM KCl; 1 mM EDTA; 0.05% digitonin; 1 mM EGTA; 1 mM PMSF, 20 μg/mL aprotinin, and 20 μg/mL leupeptin]. After a 20-minute incubation on ice, the cells were centrifuged for 10 min at 13,000 g, and the supernatant (mitochondria-free, cytosolic fraction) was recovered and frozen at -20°C for subsequent use. Enriched mitochondrial pellets were washed in ice-cold 1xPBS and then lysed in CHAPSO-buffer (5 mM $MgCl_2$; 137 mM KCl; 1 mM EDTA; 1 mM EGTA; 1% CHAPSO [3-([3-cholamidopropyl]dimethy-

lammonio)-2-hydroxy-1-propanesulfonate]; 1.4 μM pepstatin; 1 mM PMSF, 20 μg/mL aprotinin, and 20 μg/mL leupeptin). Samples were then clarified as above and supernatants isolated. Proteins from both fractions were then resolved by 12-15% SDS-PAGE and western blotted as described previously.

Cell cycle analysis and cell sorting

Cell cycle analysis was performed on ALCL cells treated with 200 nM Flavopiridol or left untreated (DMSO). The cells were washed in ice-cold 1x PBS, fixed in cold 70% ethanol, pelleted and resuspended in staining buffer (3.8 mM sodium citrate, 0.5 mg/mL RNase, 0.01 mg/mL PI) and incubated on ice, according to the manufacturer's instructions (Coulter DNA Prep™ Reagents kit; Beckam Coulter Inc., USA). Samples were analyzed on a Beckham Coulter FC500 flow cytometer. DNA histograms were analyzed using MultiCycle® for Windows (Phoenix Flow Systems, USA). To purify viable cells after 24h-treatment with flavopiridol, Karpas299 were analyzed in a FACSVantage fluorescence-activated cell sorter (Becton Dickinson), and forward (FSCA-A, Y *axes*) versus side scatter (SSC-A, X *axes*) dot plot analysis performed. As shown in Figure 5B, 30×10^3 events were analyzed after flavopiridol treatment, and the viable cells were sorted out from the apoptotic cell population or the cellular debris. The cells were then stained with PI for DNA content analysis or processed for immunofluorescence as described previously. Cell cycle analysis and immunofluorescence studies were done in parallel in intact cells sorted from untreated controls (DMSO).

Fluorescence microscopy

ALCL cells were treated with 200 nM flavopiridol or left untreated (DMSO). The cells were then spotted onto 12-well multitest slides (ICN Biomedicals, Inc., USA), fixed in 3.7% formaldehyde, permeabilized in 0.2% TritonX-100 and blocked in 100 mM glycin, followed by incubation in 10% FCS-PBS. Permeabilized cells were incubated for 1 h at 37°C with the specific primary antibodies indicated and, after washing in PBS, incubated with fluorophore-conjugated secondary antibodies Alexa488 or Alexa546, at a 1:1000 dilution of 2 mg/mL stock. Cells were then washed in PBS, mounted onto slides with 1:1 PBS/glycerol, with the addition of DAPI nucleic acid stain (1:1000). The cells were observed at 63x/0.75 NA in a Leica DMBL microscope. Images were acquired with a Leica DC 300F digital camera and prepared for reproduction with Leica IM1000 software (Leica Mycrosystem Ltd., Germany).

Mitochondrial membrane permeabilization assay

To measure changes in mitochondrial transmembrane potential ($\Delta\Psi m$), ALCL cells were treated with 200 nM flavopiridol, in the presence or in the absence of 30 μM z-vad-fmk caspase inhibitor. The cells (1×10^6) were then harvested, washed and incubated for 20 min at room temperature with 40 nM 3,3-dihexyloxacarbocyanine (DiOC6 Molecular Probes) and analyzed by flow cytometry, with excitation and emission settings of 488 nm and 525 nm, respectively. The percentage of cells exhibiting low fluorescence, reflecting loss of inner mitochondrial membrane potential, was determined by comparison with untreated controls.

Results

Flavopiridol inhibits growth and induces mitochondrial apoptosis in anaplastic large cell lymphoma cells in vitro

We first investigated the dose- and time-dependent effect of treatment with flavopiridol (25-500 nM) on the growth of human ALK-positive (Karpas299, SUDHL1) and -negative (FEPD) ALCL cells by MTT assay, assessing viability every 24 h for 3 days. Treatment with flavopiridol decreased viability in a dose- and time-dependent manner ($112.7nM\leq IC_{50}\leq169.1$ nM at 24 h; $73.9 nM\leq IC_{50}\leq153.8$ nM at 48 h; $53.2 nM\leq IC_{50}\leq109.6$ nM at 72 h), with maximal inhibition at 24 h with doses of 200 nM or higher, and more pronounced effects at later time points (Figure 1A). Dose- and time-dependent differences among ALK-positive and -negative cells in growth and survival were observed at lower concentrations of flavopiridol, with ALK-negative FEPD cells being the most sensitive among all, as confirmed by PARP cleavage analysis, a hallmark of apoptosis, and retinoblastoma (RB) state of phosphorylation, a well-known cdk downstream target, 24 h after treatment (Figure 1B). Based on these data, we selected 200 nM flavopiridol as an effective cytotoxic concentration for our study, assessing drug response as a function of time of exposure. Annexin-V staining was performed to determine apoptotic cells following drug treatment, and we found that apoptosis increased rapidly in flavopiridol-treated cells, ranging between 20% and 60% after 8 h (up to 50-90% at 24 h), with cell-type specific differences in timings of caspase-3 activation and activity as shown by immunoblot analysis (Figure 2A).

Modulation of caspase activation in flavopiridol-treated cells is determined by release of cytochrome c into the cytosol, which results from dysfunction of mitochondrial homeostasis via loss of membrane permeability after downregulation of Bcl-2 family proteins. Mcl-1 plays a significant role in maintaining mitochondrial outer membrane permeability; we, therefore, studied the effect of treatment with flavopiridol on constitutive Mcl-1 expression and transcription in ALCL cells. The immunoblot analysis revealed a significant, time-dependent decrease in Mcl-1 expression in all three cell lines following treatment with flavopiridol; this decrease strictly correlated with Mcl-1 transcriptional inhibition following cdk9-dependent RNA polymerase II dephosphorylation (Figure 2B). Under these conditions the number of cells exhibiting low uptake of lipophilic dye $DiOC_6$ increased markedly after flavopiridol treatment, being up to 80% in ALK-negative FEPD cells, and up to 30-50% in ALK-positive Karpas 299 and SUDHL1 cells (Figure 2C, graph). This was observed both in the presence and absence of z-vad-fmk caspase inhibitor, and correlated with accumulation of Bax and cytochrome c into mitochondria and the cytosol, respectively, in cells undergoing apoptosis (Figure 2C and *Online Supplementary Figure S1*).

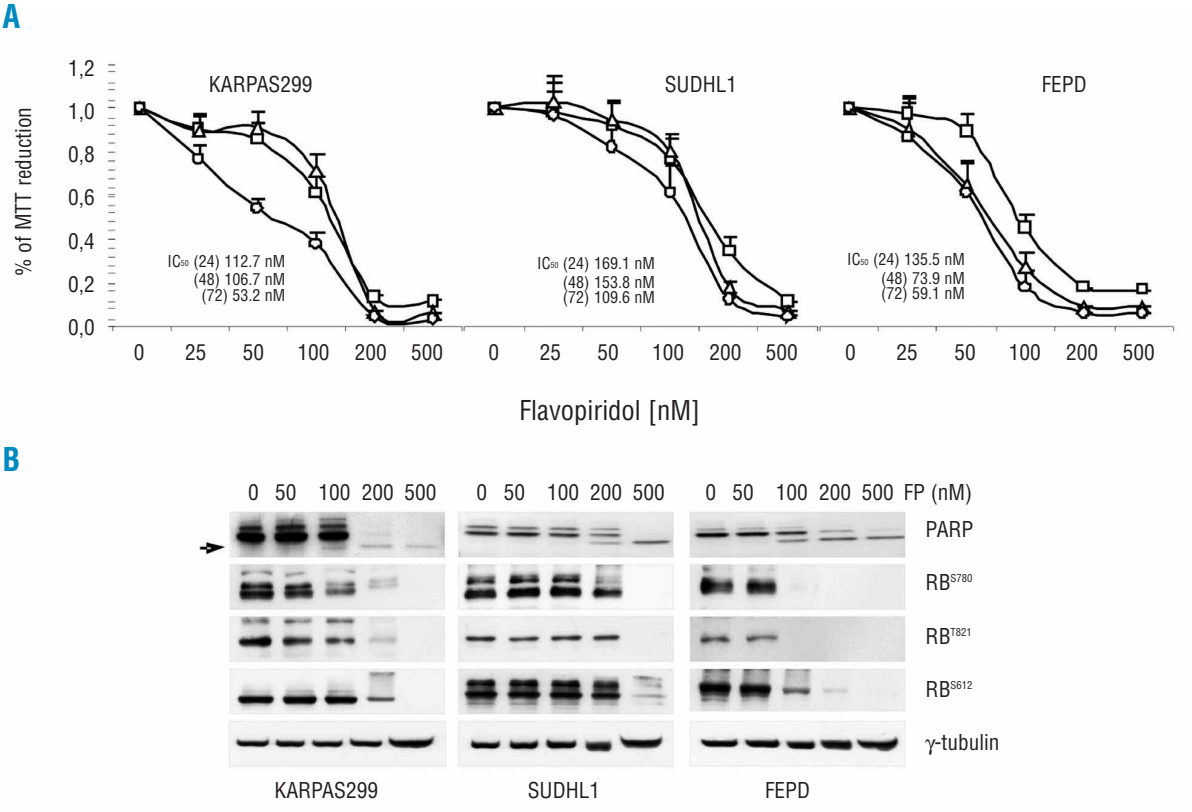

Figure 1. Dose- and time-dependent cytotoxicity profile of ALCL cells exposed to flavopiridol. (A) Exponentially growing Karpas299, SUDHL1 and FEPD cells were treated with flavopiridol (25, 50, 100, 200 and 500 nM) and cell proliferation was assessed after 24 h (□), 48 h (Δ) or 72 h (○) by MTT assay. *Points*, mean absorbance of three replicate wells, of three independent experiments, relative to untreated controls (*bars±SD*). Time-dependent dose-effect responses (IC_{50}) are reported. (B) Western blotting of 24-hour ALCL cell extracts treated with increasing concentrations of flavopiridol (50, 100, 200 and 500 nM). Steady-states of full-length PARP protein, cleaved PARP (*arrowhead*) and phosphorylated RB tumor suppressor protein were measured, and normalized to γ-tubulin for equal protein loading.

Effects of flavopiridol on cell cycle progression and regulation

To assess whether flavopiridol-induced growth inhibition and apoptosis are mediated via alterations in cell cycle, we evaluated the effect of flavopiridol on cell cycle distribution. We performed DNA cell cycle analysis using ALK-positive and -negative cells, and found that flavopiridol treatment resulted in a significant time-dependent increase of cell populations in the subG1 phase of the cell cycle, accompanied by a pronounced decrease of those in the S phase (50-90%) in the absence of cell cycle arrest (Figure 3A). In contrast, ALCL cell lines grown in the absence of the cdk inhibitor flavopiridol distributed roughly 90% of the asynchronous populations between the G1 and S phases. Nevertheless, when ALCL cells were exposed to flavopiridol for 6 or 24 h and viability measured by BrdU/7AAD incorporation into DNA, FACS analysis confirmed the time-dependent decline of S-phase cells after treatment, and the higher sensitivity of cells progressing through the S-phase to apoptosis following cdk dysfunction (Figure 3B). We also performed annexin-V analysis to demonstrate that the apoptotic population derived primarily from cells in S phase, using the DNA polymerase-inhibitor aphidicolin to synchronize cells at the G1-S boundary (Table 1) before looking at flavopiridol-induced cytotoxicity. As shown in Figure 3C, synchronized ALCL cells released into DMSO continued to grow, whereas release into flavopiridol enhanced apoptosis compared with asynchronous flavopiridol-treated cells. In particular, sequential combination of aphidicolin and flavopiridol increased cell death significantly in ALK-positive Karpas299 and SUDHL1 cells, reducing vitality 12 h after treatment to 14.5% and 26.9% respectively, compared to non-synchronized flavopiridol-treated Karpas299 and SUDHL1 cells (43.8% and 45.4%, respectively). In contrast, the percentage of viable FEPD cells remaining after flavopiridol treatment was similar both in the presence (20.7%) and absence (21.6%) of aphidicolin.

To assess whether flavopiridol-determined changes in cell cycle distribution and transcription depend on its inhibitory activity, we determined steady-state and activity of cdk after treatment. As shown in Figure 4A, flavopiridol treatment of FEPD cells caused a marked decrease in cdk protein expression (except for cdk7) in caspase-dependent and -independent manners, while the decrease in ALK-positive Karpas 299 and SUDHL1

cells was less evident with increasing time. However, using immunoblot analysis we found that treatment with flavopiridol resulted in time-dependent loss of RB^{Ser780}, RB^{Thr821} and RNA polymerase II^{Ser2} phosphorylation in all three ALCL cell lines, due to inhibition of cdk4, cdk2 and cdk9 activity (Figure 4B). In contrast, despite cdk inhibition, flavopiridol induced time-dependent phosphorylation of RB at Ser612 at early time points and binding to E2F-1, perhaps to prevent apoptosis under stress conditions (*Online Supplementary Figure S2*).[18] However, this did not prevent caspase-dependent cleavage of both partner proteins with

Table 1. Recruitment to S-phase sensitizes ALCL cells to flavopiridol. Synchronization of ALCL cells at the G1-S boundary was induced by 24h-treatment with the DNA-polymerase inhibitor aphidicolin, and confirmed by DNA content analysis by FACS.

	KARPAS299	SUDHL1	FEPD
DMSO	G1 42.7 S 49.3 G2 8.0	G1 39.7 S 42.1 G2 18.3	G1 44.7 S 35.1 G2 20.2
Aphidicolin[a]	G1 53.5 S 46.5 G2 0.0	G1 10.5 S 89.5 G2 0.0	G1 15.0 S 81.9 G2 3.1

[a] *[1.0 μg/mL] Karpas299; [0.05 μg/mL] SUDHL1; [0.1 μg/mL] FEPD.*

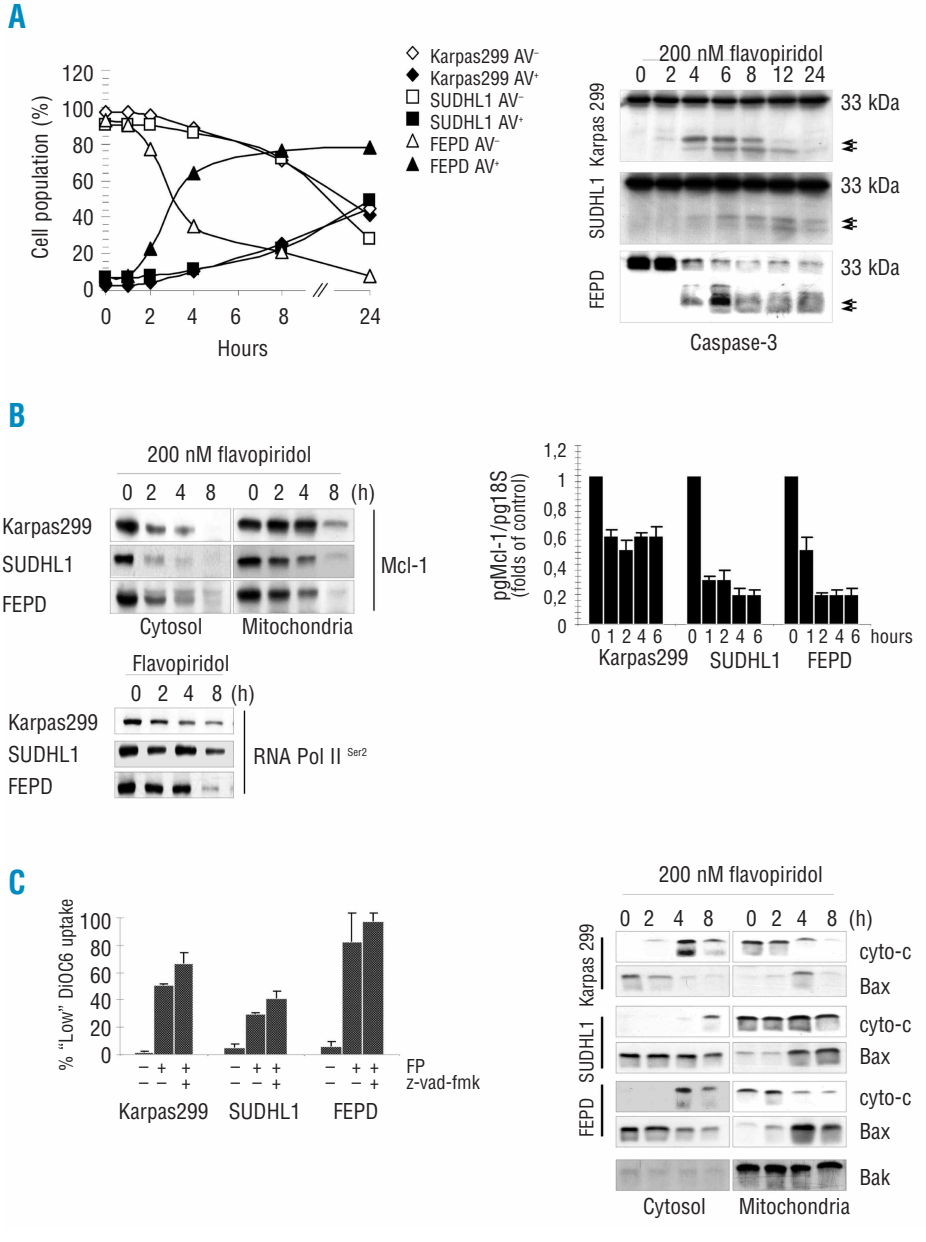

Figure 2. (A) Growing ALCL cells were treated with 200 nM flavopiridol and harvested for apoptosis assays at 1, 2, 4, 8 and 24 h. Flavopiridol-treated and untreated cells were stained with annexin-V and propidium iodide (AV/PI), and analyzed using FACS. Viable (AV^-) and apoptotic (AV^+) cells are simultaneously reported in the graph, with the sum of annexin-V-positive quadrants providing the total percentage of apoptotic cells. Time-dependent activation of caspase-3 was also assessed by western blotting, probing membranes with antibodies recognizing both full-length (33 kDa) and low molecular-weight active forms of caspase-3 (17 and 12 kDa active caspase-3, *arrowheads*). (B) Mitochondrial dysfunction in flavopiridol-treated ALCL cells. Time-course analysis of Mcl-1 protein and mRNA expression was measured by western blotting and RQ-PCR, respectively, in ALCL cells treated or not with 200 nM flavopiridol. Cytosolic and membrane-bound Mcl-1 was obtained by differential lysis with 0.05% digitonin, while Mcl-1 mRNA was obtained after the removal of endogenous DNA as described in the Design and Methods section. RQ-PCR values for each time point are expressed as the percentage of specific Mcl-1/18S mRNA, normalized to levels corresponding to those in untreated cells. Changes in phosphorylation of RNA polymerase II (RNA Pol II^{Ser2}) were also assessed as a function of time exposure and visualized by western blotting. (C) Mitochondrial membrane potential (ψm) was monitored using $DiOC_6$ lipophilic dye. ALK-positive (Karpas299 and SUDHL1) and -negative (FEPD) cells, were exposed to 200 nM flavopiridol for 24 h, with or without caspase inhibitor z-vad-fmk (30 μM).

The cells were stained with $DiOC_6$, and changes in dye uptake were analyzed by flow cytometry. The percentages of cells showing low ψm are reported in the graph, with values representing the means of separate experiments ± SD. Changes in the location of proteins involved in the maintenance of mitochondrial membrane permeability of ALCL cells were assessed by western blotting after differential lysis with digitonin. Cytosolic and mitochondrial extracts were analyzed for Bax and cytochrome c, using membrane-bound Bak as a loading control for fraction integrity.

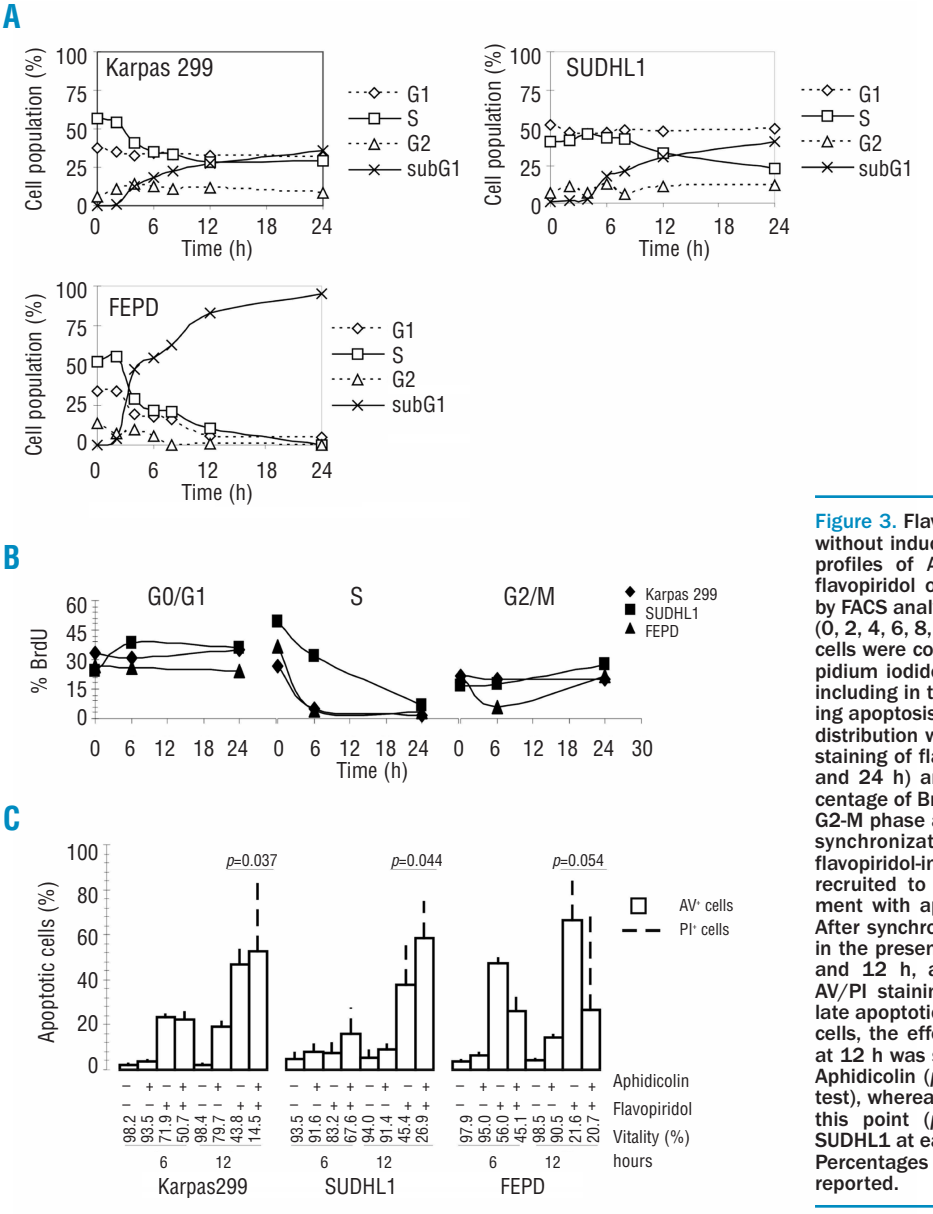

Figure 3. Flavopiridol inhibits ALCL cell survival without inducing cell cycle arrest. (A) Cell cycle profiles of ALCL cells treated with 200 nM flavopiridol or left untreated were determined by FACS analysis as a function of time exposure (0, 2, 4, 6, 8, 12 and 24 h). After treatment the cells were collected, fixed and stained with propidium iodide to determine their DNA content, including in the analysis also the cells undergoing apoptosis (SubG1). (B) Changes in cell cycle distribution were evaluated by FACS, after BrdU staining of flavopiridol-treated (200 nM for 0, 6 and 24 h) and untreated ALCL cells. The percentage of BrdU-incorporating cells in G1, S and G2-M phase are reported in the graph. (C) G1-S synchronization sensitizes ALCL cells to flavopiridol-induced apoptosis. ALCL cells were recruited to G1/S boundary after 24 h-treatment with aphidicolin as described in Table I. After synchronization ALCL cells were released in the presence or absence of flavopiridol for 6 and 12 h, and analyzed for apoptosis after AV/PI staining (AV^+, early apoptotic cells; PI^+, late apoptotic cells). In Karpas299 and SUDHL1 cells, the effect of flavopiridol with aphidicolin at 12 h was significantly less than that without Aphidicolin ($p<0.05$, determined by Student's *t* test), whereas it was not significant in FEPD at this point ($p=0.054$), or in Karpas299 and SUDHL1 at earlier time points (*data not shown*). Percentages of viable cells (vitality) are also reported.

increasing time, and cells continued to undergo apoptosis (*Online Supplementary Figure S2* and Figure 4B).

Inhibition of ALK enzymatic activity sensitizes anaplastic large cell lymphoma cells to flavopiridol-induced cell death

Accumulating evidence shows that dysregulation of several signal transduction pathways other than the cdk/cyclin pathway play an essential role in cell proliferation, survival and cell cycle control. We, therefore, evaluated the effect of flavopiridol on expression and activation of signal transducers relevant for the growth and survival of ALCL cells, such as Akt, JNK, ERK and STAT3.[19-22] Western blot analysis revealed that flavopiridol affected phosphorylation of $STAT3^{Y705}$, Akt^{S472}, $p38^{T180/Y182}$, $JNK^{T183/Y185}$, $ERK1/2^{T202/Y204}$ in ALK-negative FEPD cells because of caspase-dependent proteolysis, but not in ALK-positive cells despite the occurrence of apoptosis (Figure 4C). Indeed, phosphorylation of NPM-ALK and STAT3 was maintained in Karpas299 and SUDHL1 cells, while the levels of $JNK^{T183/Y185}$, $ERK1/2^{T202/Y204}$ and $p38^{T180/Y182}$ were increased (Figure 4C). Both ERK and JNK kinases are phosphorylated by NPM-ALK, and control cell growth. In contrast, the role of p38MAPK in ALCL cells is still unclear. In general, the ERK cascade is believed to mediate both cell proliferation and survival, whereas p38MAPK and JNK are activated in response to cellular stress. Most of the data published point to a role of p38MAP kinase activity in restraining uncontrolled cell proliferation, whereas the elevated activity of JNK mostly results in cell death. Accordingly, p38MAPK inhibits G1/S or G2/M transition by differential regulation of cdk target proteins, such as $p21^{WAF}$ and Cdc25, and JNK affects cell survival

through deregulation of Bcl-2 family member proteins and mitochondrial dysfunction.[23,24] However, depending on the cell type, the threshold for activation of MAP kinases may be different in response to stress, and thus also the propensity of cells to undergo cell cycle arrest or apoptosis. In NPM-ALK positive cells we observed an increase of ERK, JNK and p38MAPK phosphorylation both in cells undergoing apoptosis and arrested at G1-phase after flavopiridol treatment (Figure 4C and D). However, activation of p38MAPK was dramatic mostly after cell cycle arrest (Figure 4D, western blotting), whereas ERK1/2 and JNK1/2 phosphorylation increased

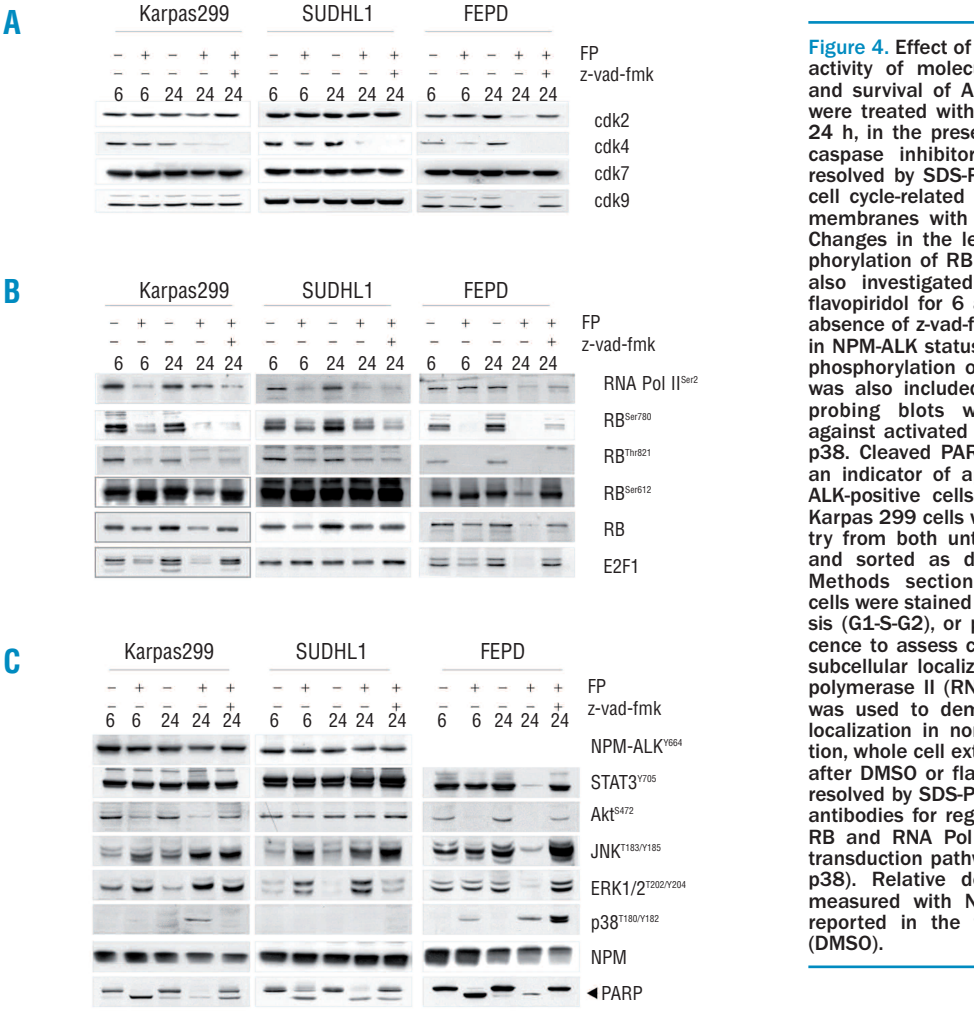

Figure 4. Effect of flavopiridol on expression and activity of molecular determinants of growth and survival of ALCL cells. (A) ALCL cell lines were treated with 200 nM flavopiridol for 6 or 24 h, in the presence or absence of z-vad-fmk caspase inhibitor. Whole cell extracts were resolved by SDS-PAGE, and the steady-state of cell cycle-related proteins assessed by probing membranes with the indicated antibodies. (B) Changes in the levels of expression and phosphorylation of RB and RNA polymerase II were also investigated in ALCL cells exposed to flavopiridol for 6 and 24 h, in the presence or absence of z-vad-fmk inhibitor, as were changes in NPM-ALK status and activity (C). The state of phosphorylation of different signal transducers was also included as described in the figure, probing blots with site-specific antibodies against activated STAT3, Akt, JNK, ERK1/2 and p38. Cleaved PARP (arrowheads) was used as an indicator of apoptosis. (D) To purify viable ALK-positive cells after flavopiridol treatment, Karpas 299 cells were analyzed by flow cytometry from both untreated and treated samples, and sorted as described in the Design and Methods section. Flavopiridol-treated viable cells were stained with PI for DNA content analysis (G1-S-G2), or processed for immunofluorescence to assess chromatin integrity (DAPI) and subcellular localization of phosphorylated RNA polymerase II (RNA Pol II). Cdk9 inhibitor DRB was used to demonstrate RNA polymerase II localization in non-transcribing nuclei. In addition, whole cell extracts of viable cells recovered after DMSO or flavopiridol (FP) treatment were resolved by SDS-PAGE, and probed with specific antibodies for regulators of the cell cycle (cdk, RB and RNA Pol II) and the NPM-ALK signal transduction pathway (STAT3, JNK, ERK1/2 and p38). Relative densities of the bands were measured with NIH Image software and are reported in the figure as fold(s) of controls (DMSO).

D

	DMSO (–)		Flavopiridol (+)	
	# Events	% Total	# Events	% Total
Total	30.000	100.0	30.000	100.0
Viable cells	28.728	95.8	8.773	29.2
Cell phase				
G1		35.7		63.9
S		50.6		18.9
G2		13.7		17.2

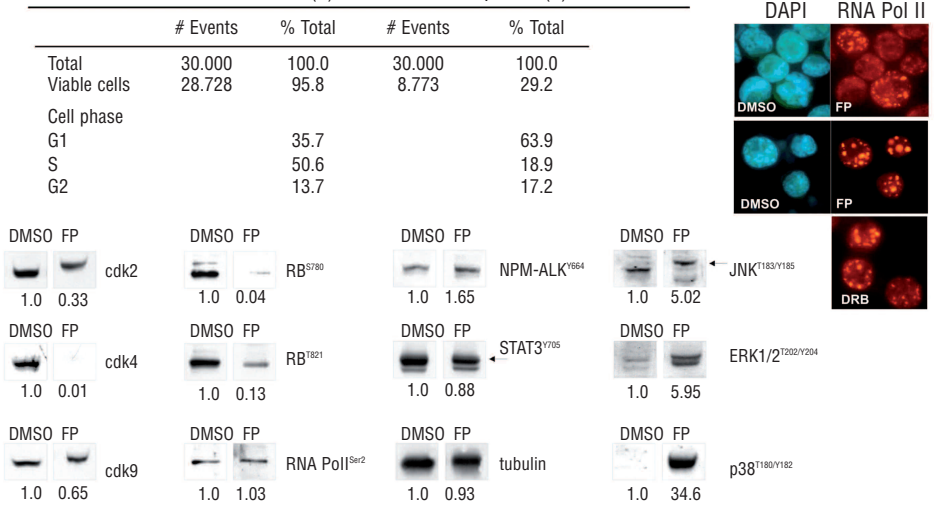

mostly in apoptotic cells (Figure 4C). Besides, downregulation of cdk activity in G1-arrested cells was still observed, as was the accumulation of inactive RNA polymerase II in dot-like structures typical of transcriptionally inhibited cells,[25] suggesting that flavopiridol uptake and inhibitory activity were unaffected (Figure 4D, western blotting and immunofluorescence). Whether the phosphorylation of MAP kinases is involved in the regulation of flavopiridol-induced apoptosis, or simply a secondary response to deregulation of signaling, is not known. However, when used in combination with flavopiridol, p38 MAPK inhibitor, SB202190, but not JNK and ERK inhibitors SP600125 and PD98059, caused a robust increase in annexin V staining, suggesting a possible negative effect of phosphorylated p38 MAPK on flavopiridol-mediated apoptosis (*unpublished data*).

To assess whether flavopiridol-induced apoptosis was NPM-ALK dependent, we next examined the role of NPM-ALK on drug response, measuring apoptosis in the presence or absence of the ALK small-molecule inhibitor WHI-154.[26,27] As shown in Figure 5A, expression of NPM-ALK^{Y664} in Karpas299 cells was inhibited by WHI-154 in a dose-dependent manner, under conditions that reduced stability of the total protein without cytotoxic effects (*see below*). Inhibition of key signaling proteins was concentration-dependent and showed a strong correlation with NPM-ALK inactivation. As expected, phos-

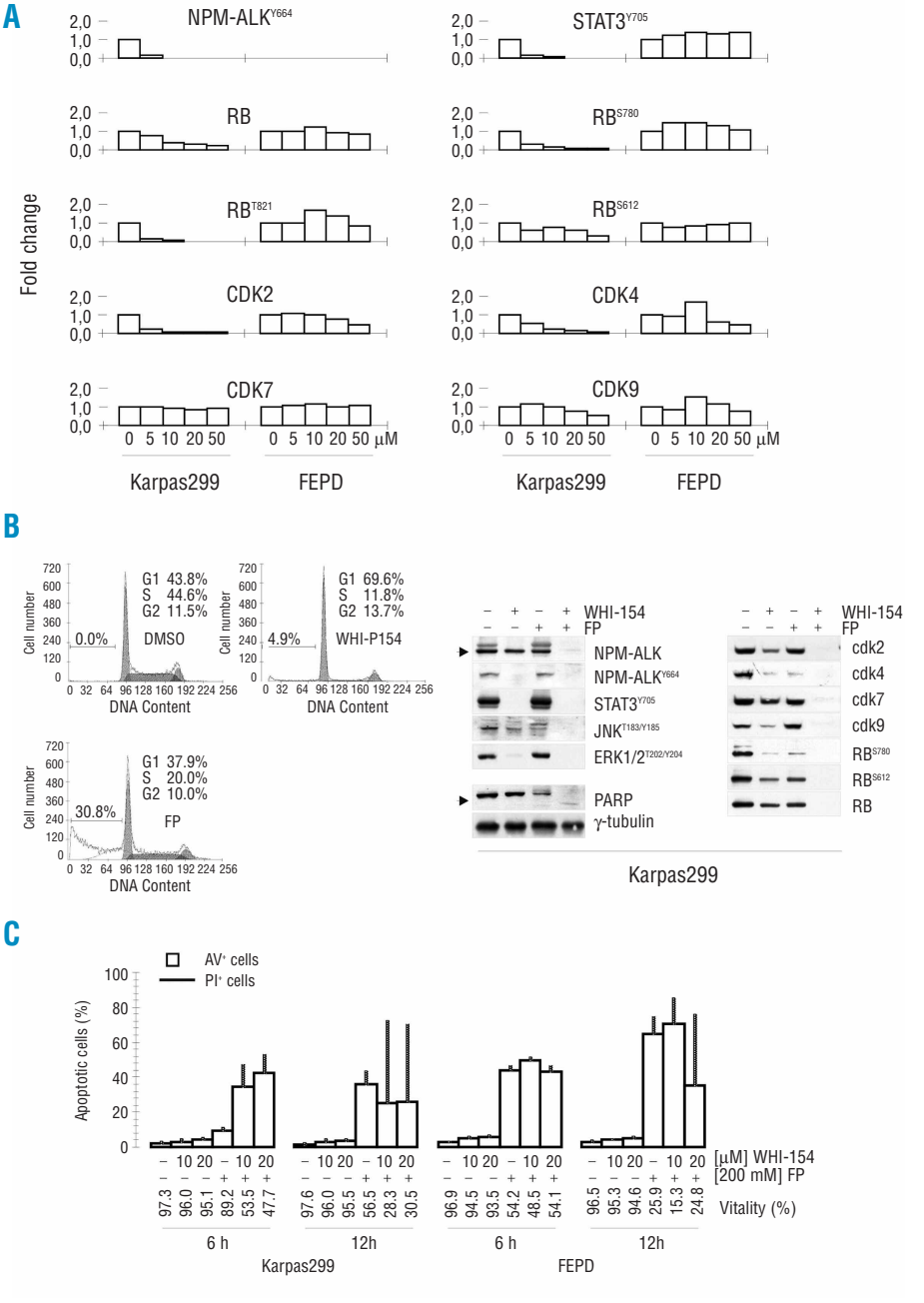

Figure 5. WHI-154 inhibitor-mediated suppression of NPM-ALK tyrosine kinase activity. (A) To evaluate expression of phospho-NPM-ALK (NPM-ALK^{Y664}), as well as changes in the levels of expression and degree of phosphorylation of NPM-ALK-related or -unrelated downstream signaling proteins, ALK-positive and -negative, Karpas299 and FEPD cells respectively, were treated with 5, 10, 20 and 50 μM WHI-154 for 24 h, or left untreated. Total cell lysates were prepared as described in the Design and Methods section, and resolved by SDS-PAGE. Blots were probed for the proteins indicated, and relative densities of the bands were measured with NIH Image software and normalized to untreated controls. (B) Combined treatment with flavopiridol and WHI-154 markedly enhances the downregulation of proteins involved in growth and survival of ALCL cells. Karpas299 cells were exposed to 200 nM flavopiridol±20 μM WHI-154 for 24 h. Thirty mg of proteins of whole cell lysates from treated and untreated samples were resolved by SDS-PAGE and analyzed by western blotting for the proteins indicated in the figure. Blots were stripped and probed for γ-tubulin to ensure equivalent loading and transfer. Karpas299 cells, untreated or treated with flavopiridol or WHI-154 were also stained with PI for DNA content analysis of diploid and sub-diploid cells. (C) Striking potentiation of apoptosis in ALCL cells co-exposed to flavopiridol and WHI-154. Karpas299 and FEPD cells were treated with WHI-154 for 12 h, prior to addition of flavopiridol (200 nM) for the indicated time periods (6 and 12 h). After treatment the cells were stained with annexin-V and propidium iodide for apoptosis analysis by FACS. Percentages of early apoptotic (AV$^+$), late apoptotic (PI$^+$) and viable cells (vitality) are reported.

phorylation of STAT3 was strongly impaired, but so too was the expression of cdk2, cdk4 and cdk-phosphorylated RB, whereas cdk7 and cdk9 levels were mostly unaffected (Figure 5A). In contrast, changes of protein expression in ALK-negative FEPD cells treated with WHI-154 were not significant. At concentrations for which complete inhibition of NPM-ALK autophosphorylation was observed, WHI-154 caused G1 cell cycle arrest in the absence of apoptosis in ALK-positive Karpas299 cells, whereas perturbations of the cell cycle by flavopiridol reflected the induction of apoptosis previously demonstrated (Figure 5B). The advantage of a combination of these drugs was, therefore, investigated, and compared to the ability of single agents to perturb the expression of proteins critical for signaling ($STAT3^{Y705}$, $JNK^{T183/Y185}$, $ERK1/2^{T202/Y204}$), growth (cyclin A and B1, cdk2 and 4, $p27^{Kip}$, RB^{S780} and RB^{S612}) and survival (PARP). As shown by immunoblot analysis, upon co-administration of WHI-154 with flavopiridol, all regulators of proliferation and survival were totally depleted from ALCL cells, including active NPM-ALK^{Y664}, activated $STAT3^{Y705}$, $JNK^{T183/Y185}$ and $ERK1/2^{T202/Y204}$, and apoptosis was strongly induced as shown by PARP cleavage analysis (Figure 5B). When cells were stained with annexin-V and examined by FACS, apoptosis was enhanced in WHI-154/flavopiridol-treated Karpas299 cells, but not in ALK-negative FEPD cells (Figure 5C). When used alone, WHI-154 did not cause apoptosis in either ALK-positive or -negative ALCL cells. When WHI-154 was added to flavopiridol, however, flavopiridol-dependent apoptosis increased in Karpas299 cells from 11% to ~50% after 6 h, and from 44% to ~70% 12 h post-treatment, indicating the role of NPM-ALK in modulating tumor cell responsiveness to cdk inhibition. Conversely, the combined treatment had minimal effects in FEPD cells, and apoptosis was mainly due to flavopiridol (~45% and ~75%, at 6 and 12h in flavopiridol-treated cells; ~48% and ~80% in flavopiridol/WHI-154-treated cells).

Discussion

Cyclin-dependent kinases are attractive targets for drug development since their activity, required for the correct timing and ordering of the cell cycle, is frequently deregulated in cancer.[28] Numerous small molecule inhibitors of cdk have been identified and proven effective in treating tumors, based on the increased sensitivity of the transformed cells to changes in the levels and activity of cdk.[29,30] However the consequences of cdk inactivation are complex and can result in disparate outcomes depending on the tumor type and the genetic context that drives their expression. Besides, cdk inhibition *per se* is not sufficient for selective tumor cell killing, and relies on changes in the activity of signal transduction pathways critical for survival, or in the balance of pro- and anti-apoptotic signals.[31] Competitive inhibitors of both cell-cycle and transcriptional cdk exert a more potent antitumor activity in different preclinical models than compounds with selective cdk inhibitory activity, due perhaps to the functional compensation between cdk family members.[32-35] Tumor cells engineered to silence cdk2 do not necessarily arrest or die, as they may compensate for lower cdk2 activity with cdk1 or cdk4/6, while cell-cycle arrest caused by combined depletion of cdk1 and cdk2 likely results in cell death, occurring even more rapidly if other cdk are concomitantly impaired.[36-39] As ALCL cells proliferate rapidly and cell cycle deregulation has recently been shown to contribute to lymphomagenesis, we investigated whether targeting the cyclin/cdk axis could inhibit tumor growth, and assessed this hypothesis using the multiple cdk inhibitor flavopiridol, alone or combined with NPM-ALK kinase inhibitors.

ALCL is a highly aggressive subtype of non-Hodgkin's lymphoma characterized by expression and constitutive activity of the NPM-ALK tyrosine kinase. NPM-ALK controls functional activation of both upstream regulators (RAS, ERK1/2, JNK and AKT) and downstream effector proteins (Myc, c-Jun, Fos, and STAT3/5) of ALCL signaling, and has direct or indirect activity on growth, survival, migration and cell shaping.[17] Consistently, a differential expression and activation of various regulatory proteins, including D-type cyclins, cyclins A and E, as well as cdk inhibitors $p21^{WAF}$, $p27^{Kip}$ and RB has been observed in NPM-ALK-expressing cells, as a result of enhanced AP-1, STAT3 or MYC transcriptional activity by JNK and ERK kinases, or reduced FOXO3A activity by AKT.[27,40-42] We proved here that cdk inactivation leads to mitochondrial damage, caspase activation and apoptosis in ALCL cells, in time- and dose-dependent manners, through inhibition of DNA synthesis and RNA transcription, selective killing of S-phase cells, and the engagement of different growth-inhibitory pathways. Our study revealed that ALCL cells do not display cell cycle arrest in the presence of flavopiridol, but undergo preferential death of the S-phase population at drug concentrations that correlate with cdk inhibition. They stall in G1 or G2-M phase when apoptosis is prevented by *z*-vad-fmk caspase inhibitor, whereas they die rapidly when allowed to enter S phase after recruitment to G1/S boundary. Due to flavopiridol inhibitory activity, RB tumor suppressor protein was dephosphorylated at cdk sites Ser780 and Thr821, and associated with E2F1 early after drug addition, before caspase-dependent cleavage. Cdk inhibition also reduced phosphorylation and transcriptional activity of RNA polymerase II, causing a concomitant decrease in protein expression, likely due to degradation of the enzyme.

The transcripts most sensitive to reduced RNA polymerase II phosphorylation are those with short half-lives, including transcripts encoding anti-apoptotic proteins. Depletion of the corresponding proteins in response to the inhibition of transcriptional cdks (i.e. cdk9) may induce cell death and, in some instances, may sensitize cells to other apoptotic stimuli. In this context, flavopiridol caused strong inhibition of Mcl-1 transcription and expression in ALCL cells, which resulted in the collapse of mitochondrial membrane potential. When Mcl-1 expression was abolished, pro-apoptotic Bax protein accumulated at mitochondria,

and release of cytochrome c into the cytoplasm correlated with caspase-3 activation.

Known advantages of cdk inhibition are unrestrained E2F-1 activity during S phase which leads to aberrant expression of pro-apoptotic genes and predisposes cells to death, as well as reduced regulatory phosphorylation of RNA polymerase II which affects short half-life transcripts of rapidly turned-over anti-apoptotic proteins.[43-45] Nonetheless, problems of this approach can be factors that favor cell cycle arrest over apoptosis, such as functional RB, EGFR and AKT, which impede E2F1-mediated apoptosis, or JNK and ERK1/2 kinases, which affect transcription and expression of anti-apoptotic proteins. We, therefore, looked at additional events contributing to flavopiridol antitumor activity, assessing the steady-state of primary downstream mediators of NPM-ALK transforming activity in ALCL, whose inhibition improves flavopiridol cytotoxicity as recently shown.[46,47] We found that ALCL cells treated with flavopiridol alone did not display a significant decline in NPM-ALK protein expression and activity, and exhibited a pronounced activation of ERK1/2 and JNK kinases, not observed in ALK-negative ALCL cells. Consistently, differences in the extent and time of flavopiridol-induced apoptosis were observed between the ALK-negative and -positive cell lines, with the latter also showing viable cells after treatment. These cells, when isolated, were found to maintain NPM-ALK status and activity despite the downregulation of cdk activity, which ruled out any lack of flavopiridol activity because of differential drug saturation or efflux, though suggesting a context-dependent model able to modulate drug effectiveness and sensitivity in ALK-positive cells.[48]

The possibility that the interruption of NPM-ALK signaling could increase the response to flavopiridol was investigated by targeting NPM-ALK, as shown with other oncogenic kinases.[30,49,50] Our study demonstrated that the cytoreductive activity of the NPM-ALK small-molecule inhibitor WHI-154 resulted in downregulation of cell cycle-related proteins, including cdk, as well as in near-complete depletion of NPM-ALK-activated downstream signal proteins. This led to cell cycle arrest in the absence of apoptosis when WHI-154 was used as a single agent, whereas it caused an increase in cell death when administered with the cdk-inhibitor flavopiridol. The onset of apoptosis was extremely fast and robust with the combination of those two drugs, perhaps due to enhanced efficacy on the molecular determinants controlling proliferation and survival of ALCL cells. Pharmacological interruption of NPM-ALK signaling dramatically lowered the ALCL threshold for caspase activation by flavopiridol, proving the critical role of the oncogenic kinase in preventing drug-induced apoptosis. These cells became particularly vulnerable when cell cycle and survival signal events were simultaneously disrupted, strengthening the hypothesis that targeting cyclin/cdk signaling is an effective anti-tumor approach against ALCL, and supporting the evidence that, in combination with NPM-ALK inhibition, this strategy is even more promising in ALK-positive malignancies.

Authorship and Disclosures

PB: performed and designed the research, analyzed the data and wrote the paper. EZ, GM and MP: performed the research. LM: performed the research and contributed to analysis of the data. GB: co-ordinated the fluorocytometric analysis and provided critical evaluation of results. AR: designed and co-ordinated the research, analyzed the data and wrote the paper.

The authors reported no potential conflicts of interest.

References

1. Vermeulen K, Van Bockstaele DR, Berneman ZN. The cell cycle: a review of regulation, deregulation and therapeutic targets in cancer. Cell Prolif 2003;36:131-49.
2. Novak B, Tyson JJ, Gyorffy B, Csikasz-Nagy A. Irreversible cell-cycle transitions are due to systems-level feedback. Nat Cell Biol 2007;9:724-8.
3. Massague J. G1 cell-cycle control and cancer. Nature 2004;432:298-306.
4. Oelgeschlager T. Regulation of RNA polymerase II activity by CTD phosphorylation and cell cycle control. J Cell Physiol 2002;190:160-9.
5. Shapiro GI. Cyclin-dependent kinase pathways as targets for cancer treatment. J Clin Oncol 2006;24:1770-83.
6. Berthet C, Kaldis P. Cell-specific responses to loss of cyclin-dependent kinases. Oncogene 2007;26:4469-77.
7. Besson A, Dowdy SF, Roberts JM. CDK inhibitors: cell cycle regulators and beyond. Dev Cell 2008;14:159-69.
8. Swanton C. Cell-cycle targeted therapies. Lancet Oncol 2004;5:27-36.
9. Malumbres M, Pevarello P, Barbacid M, Bischoff JR. CDK inhibitors in cancer therapy: what is next? Trends Pharmacol Sci 2008;29:16-21.
10. Senderowicz AM. Small-molecule cyclin-dependent kinase modulators. Oncogene 2003;22:6609-20.
11. Sedlacek HH. Mechanisms of action of flavopiridol. Crit Rev Oncol Hematol 2001;38:139-70.
12. Shapiro GI. Preclinical and clinical development of the cyclin-dependent kinase inhibitor flavopiridol. Clin Cancer Res 2004;10:4270s-5s.
13. Grant S, Dent P. Gene profiling and the cyclin-dependent kinase inhibitor flavopiridol: what's in a name? Mol Cancer Ther 2004;3:873-5.
14. Chen R, Keating MJ, Gandhi V, Plunkett W. Transcription inhibition by flavopiridol: mechanism of chronic lymphocytic leukemia cell death. Blood 2005;106:2513-9.
15. Bischof D, Pulford K, Mason DY, Morris SW. Role of the nucleophosmin (NPM) portion of the non-Hodgkin's lymphoma-associated NPM-anaplastic lymphoma kinase fusion protein in oncogenesis. Mol Cell Biol 1997;17:2312-25.
16. Morris SW, Kirstein MN, Valentine MB, Dittmer KG, Shapiro DN, Saltman DL, Look AT. Fusion of a kinase gene, ALK, to a nucleolar protein gene, NPM, in non-Hodgkin's lymphoma. Science 1994;263:1281-4.
17. Chiarle R, Voena C, Ambrogio C, Piva R, Inghirami G. The anaplastic lymphoma kinase in the pathogenesis of cancer. Nat Rev Cancer 2008;8:11-23.
18. Inoue Y, Kitagawa M, Taya Y. Phosphorylation of pRB at Ser612 by Chk1/2 leads to a complex between pRB and E2F-1 after DNA damage. Embo J 2007;26:2083-93.
19. Dai Y, Rahmani M, Grant S. Proteasome inhibitors potentiate leukemic cell apoptosis induced by the cyclin-dependent kinase

inhibitor flavopiridol through a SAPK/JNK- and NF-κB-dependent process. Oncogene 2003;22:7108-22.
20. Gomez LA, de Las Pozas A, Perez-Stable C. Sequential combination of flavopiridol and docetaxel reduces the levels of X-linked inhibitor of apoptosis and AKT proteins and stimulates apoptosis in human LNCaP prostate cancer cells. Mol Cancer Ther 2006;5:1216-26.
21. Kim DM, Koo SY, Jeon K, Kim MH, Lee J, Hong CY, Jeong S. Rapid induction of apoptosis by combination of flavopiridol and tumor necrosis factor (TNF)-alpha or TNF-related apoptosis-inducing ligand in human cancer cell lines. Cancer Res 2003;63:621-6.
22. Takada Y, Sethi G, Sung B, Aggarwal BB. Flavopiridol suppresses tumor necrosis factor-induced activation of activator protein-1, c-Jun N-terminal kinase, p38 mitogen-activated protein kinase (MAPK), p44/p42 MAPK, and Akt, inhibits expression of antiapoptotic gene products, and enhances apoptosis through cytochrome c release and caspase activation in human myeloid cells. Mol Pharmacol 2008;73:1549-57.
23. Kim BS, Yoon KH, Oh HM, Choi EY, Kim SW, Han WC, et al. Involvement of p38 MAP kinase during iron chelator-mediated apoptotic cell death. Cell Immunol 2002; 220:96-106.
24. Shukla S, Gupta S. Apigenin-induced cell cycle arrest is mediated by modulation of MAPK, PI3K-Akt, and loss of cyclin D1 associated retinoblastoma dephosphorylation in human prostate cancer cells. Cell Cycle 2007;6:1102-14.
25. Bregman DB, Du L, van der Zee S, Warren SL. Transcription-dependent redistribution of the large subunit of RNA polymerase II to discrete nuclear domains. J Cell Biol 1995; 129:287-98.
26. Sudbeck EA, Liu XP, Narla RK, Mahajan S, Ghosh S, Mao C, et al. Structure-based design of specific inhibitors of Janus kinase 3 as apoptosis-inducing antileukemic agents. Clin Cancer Res 1999;5:1569-82.
27. Marzec M, Kasprzycka M, Ptasznik A, Wlodarski P, Zhang Q, Odum N, et al. Inhibition of ALK enzymatic activity in T-cell lymphoma cells induces apoptosis and suppresses proliferation and STAT3 phosphorylation independently of Jak3. Lab Invest 2005;85:1544-54.
28. Malumbres M, Barbacid M. Cell cycle kinases in cancer. Curr Opin Genet Dev 2007;17:60-5.
29. Hahntow IN, Schneller F, Oelsner M, Weick K, Ringshausen I, Fend F, et al. Cyclin-dependent kinase inhibitor roscovitine induces apoptosis in chronic lymphocytic leukemia cells. Leukemia 2004;18: 747-55.
30. Wang L, Wang J, Blaser BW, Duchemin AM, Kusewitt DF, Liu T, et al. Pharmacologic inhibition of CDK4/6: mechanistic evidence for selective activity or acquired resistance in acute myeloid leukemia. Blood 2007;110:2075-83.
31. Collins I, Garrett MD. Targeting the cell division cycle in cancer: CDK and cell cycle checkpoint kinase inhibitors. Curr Opin Pharmacol 2005;5:366-73.
32. Gao N, Kramer L, Rahmani M, Dent P, Grant S. The three-substituted indolinone cyclin-dependent kinase 2 inhibitor 3-[1-(3H-imidazol-4-yl)-meth-(Z)-ylidene]-5-methoxy-1,3-dihydro-indol-2-one (SU9516) kills human leukemia cells via down-regulation of Mcl-1 through a transcriptional mechanism. Mol Pharmacol 2006;70:645-55.
33. Jackman KM, Frye CB, Hunger SP. Flavopiridol displays preclinical activity in acute lymphoblastic leukemia. Pediatr Blood Cancer 2008;50:772-8.
34. Smith ME, Cimica V, Chinni S, Challagulla K, Mani S, Kalpana GV. Rhabdoid tumor growth is inhibited by flavopiridol. Clin Cancer Res 2008; 14:523-32.
35. Zhang C, Lundgren K, Yan Z, Arango ME, Price S, Huber A, et al. Pharmacologic properties of AG-012986, a pan-cyclin-dependent kinase inhibitor with antitumor efficacy. Mol Cancer Ther 2008;7:818-28.
36. Martín A, Odajima J, Hunt SL, Dubus P, Ortega S, Malumbres M, Barbacid M. Cdk2 is dispensable for cell cycle inhibition and tumor suppression mediated by p27(Kip1) and p21(Cip1). Cancer Cell 2005;7:591-8.
37. Berthet C, Kaldis P. Cdk2 and Cdk4 cooperatively control the expression of Cdc2. Cell Div 2006;1:10.
38. Cai D, Latham VM Jr, Zhang X, Shapiro GI. Combined depletion of cell cycle and transcriptional cyclin-dependent kinase activities induces apoptosis in cancer cells. Cancer Res 2006;66:9270-80.
39. Malumbres M, Sotillo R, Santamaría D, Galán J, Cerezo A, Ortega S, et al. Mammalian cells cycle without the D-type cyclin-dependent kinases Cdk4 and Cdk6. Cell 2004;118:493-504.
40. Marzec M, Kasprzycka M, Liu X, Raghunath PN, Wlodarski P, Wasik MA. Oncogenic tyrosine kinase NPM/ALK induces activation of the MEK/ERK signaling pathway independently of c-Raf. Oncogene 2007; 26:813-21.
41. Staber PB, Vesely P, Haq N, Ott RG, Funato K, Bambach I, et al. The oncoprotein NPM-ALK of anaplastic large-cell lymphoma induces JUNB transcription via ERK1/2 and JunB translation via mTOR signaling. Blood 2007;110:3374-83.
42. Vega F, Medeiros LJ, Leventaki V, Atwell C, Cho-Vega JH, Tian L, et al. Activation of mammalian target of rapamycin signaling pathway contributes to tumor cell survival in anaplastic lymphoma kinase-positive anaplastic large cell lymphoma. Cancer Res 2006;66:6589-97.
43. Jiang J, Matranga CB, Cai D, Latham VM Jr, Zhang X, Lowell AM, et al. Flavopiridol-induced apoptosis during S phase requires E2F-1 and inhibition of cyclin A-dependent kinase activity. Cancer Res 2003;63:7410-22.
44. Litz J, Carlson P, Warshamana-Greene GS, Grant S, Krystal GW. Flavopiridol potently induces small cell lung cancer apoptosis during S phase in a manner that involves early mitochondrial dysfunction. Clin Cancer Res 2003;9:4586-94.
45. Matranga CB, Shapiro GI. Selective sensitization of transformed cells to flavopiridol-induced apoptosis following recruitment to S-phase. Cancer Res 2002;62:1707-17.
46. Lee YK, Isham CR, Kaufman SH, Bible KC. Flavopiridol disrupts STAT3/DNA interactions, attenuates STAT3-directed transcription, and combines with the Jak kinase inhibitor AG490 to achieve cytotoxic synergy. Mol Cancer Ther 2006; 5:138-48.
47. Yu C, Rahmani M, Dai Y, Conrad D, Krystal G, Dent P, Grant S. The lethal effects of pharmacological cyclin-dependent kinase inhibitors in human leukemia cells proceed through a phosphatidylinositol 3-kinase/Akt-dependent process. Cancer Res 2003;63:1822-33.
48. Chau BN, Wang JY. Coordinated regulation of life and death by RB. Nat Rev Cancer 2003;3:130-8.
49. Phillip CJ, Stellrecht CM, Nimmanapalli R, Gandhi V. Targeting MET transcription as a therapeutic strategy in multiple myeloma. Cancer Chemother Pharmacol 2009;63:587-97.
50. Sambol EB, Ambrosini G, Geha RC, Kennealey PT, Decarolis P, O'Connor R, et al. Flavopiridol targets c-KIT transcription and induces apoptosis in gastrointestinal stromal tumor cells. Cancer Res 2006;66: 5858-66.